Please cite the Published Version

Additional Information: This is an open access article which first appeared in Future Generation Computer Systems

Data Access Statement: No data was used for the research described in the article.

An intelligent resource allocation strategy with slicing and auction for private edge cloud systems

Yuhuai Peng [a], Jing Wang [a], Xiongang Ye [a], Fazlullah Khan [b],*, Ali Kashif Bashir [c,d,e], Bandar Alshawi [f], Lei Liu [g], Marwan Omar [h]

[a] *School of Computer Science and Engineering, Northeastern University, Shenyang 110819, China*
[b] *School of Computer Science, Faculty of Science and Engineering, University of Nottingham Ningbo China, Ningbo 315104, Zhejiang, China*
[c] *Department of Computer Networks and Cybersecurity, Manchester Metropolitan University, UK*
[d] *Department of Computer Science and Mathematics, Lebanese American University, Beirut, Lebanon*
[e] *Woxsen School of Business, Woxsen University, Hyderabad, 502 345, India*
[f] *Department of Computer and Network Engineering, College of Computing, Umm Al-Qura University, Makkah, Saudi Arabia*
[g] *Guangzhou Institute of Technology, Xidian University, Guangzhou 510555, China*
[h] *Information Technology and Management, Illinois Institute of Technology, USA*

ARTICLE INFO

ABSTRACT

The convergence of transformative technologies, including the Internet of Things (IoT), Big Data, and Artificial Intelligence (AI), has driven private edge cloud systems to the forefront of research efforts. The access to massive terminals and the emergence of personalized services pose serious challenges for efficient resource management in power private edge cloud systems. To address the challenge of inequitable resource allocation in the private edge cloud, this work proposes an intelligent resource allocation strategy with a slicing and auction approach. By formalizing the resource allocation problem as a Mixed Integer Nonlinear Programming (MINLP) puzzle, the method transforms it into a hierarchical allocation challenge for Mobile Network Operators (MNOs), Mobile Virtual Network Operators (MVNOs), and power terminals. The proposed Multi-hop Progressive Auction Algorithm (MPAA) addresses the sliced resource allocation problem between MNOs and MVNOs. Furthermore, a Terminal Resource Allocation Strategy (TRAS) based on improved particle swarm optimization is proposed to solve the spectrum resource allocation problem between MVNOs and power terminals. Extensive simulation results show that the bidding overhead of MPAA is reduced by 6.12% and the average terminal satisfaction of TRAS is improved by about 1.3% compared to conventional methods, thus improving the utilization of wireless resources within the power AIoT.

1. Introduction

By seamlessly integrating Information and Communication Technology (ICT) and power infrastructure, the power Artificial Intelligence of Things (AIoT) enhances the operational efficiency, reliability, intelligence, and interaction of the grid [1–3]. As a customized component of power AIoT, private edge cloud systems ensure real-time monitoring, rapid response to faults, remote control of the grid, and other instantaneous operations by dynamically allocating computing, storage, and network resources [4]. Massive access to smart wireless terminals used for power distribution, transmission, and management, causes exponential growth in data volume. The private edge cloud network makes it difficult to meet the tight demands of low latency for smart services [5,6]. Spectrum allocation directly determines the speed and quality of data transmission from terminal devices to the private edge cloud. It is the core of providing ultra-low latency and high bandwidth communication services in power private edge cloud systems. Therefore, efficient wireless resource slicing and reasonable spectrum allocation are of great significance in improving the service quality of private edge cloud systems.

In the context of the power private edge cloud systems, certain intelligent services depend on high bandwidth and low latency transmission, including highly reliable distribution network protection, robotic inspection, and other control-class functionalities [7]. Intelligent services are increasing with the growing access to smart terminals. Secondly, Smart meters, various types of power monitoring sensors, and other massively connected devices generate massive amounts of collected

---

data to be transmitted. The heterogeneous devices highlight the demand for differentiated and personalized spectrum resource allocation strategies [8]. In addition, the spatial and temporal complexity of services is increasing due to changing user demands. Consequently, the multiple services offered by the power private edge cloud systems pose a significant challenge to allocating spectrum resources.

Numerous researchers have studied the wireless spectrum allocation problem and established it as a non-convex mixed-integer programming problem. This complex problem is converted into a combinatorial optimization problem [9]. Various methods have been used to solve this problem, including greedy algorithms, machine learning, and dynamic programming algorithms, but often only local optima are obtained. Particularly noteworthy among these strategies are auction algorithms, which efficiently allocate spectrum resources while maximizing auction revenues [10]. It is characterized by low computational complexity and fast convergence. However, the currently prevailing spectrum auction algorithm is mainly centralized and not directly applicable to complex grids.

To solve the problem of inequality in wireless resource allocation in local power AIoT, we propose an intelligent resource allocation strategy with slicing and auction for private edge cloud systems. The main contributions of this research can be described as follows:

1. The resource allocation problem is formalized and elucidated as a mixed-integer nonlinear programming problem. The Multi-hop Progressive Auction Algorithm (MPAA) is introduced to address the complex task of resource allocation between Mobile Network Operators (MNOs) and Mobile Virtual Network Operators (MVNOs).
2. A Terminal Resource Allocation Strategy (TRAS) is proposed to address the challenge of spectrum resource allocation between MVNOs and power terminals, using an improved Particle Swarm Optimization (PSO). To prevent convergence to local optima, a simulated annealing algorithm is integrated to enhance the global search capabilities of the PSO.
3. Extensive simulations demonstrate that MPAA effectively mitigates unnecessary costs associated with overpricing. Comparative analysis with conventional algorithms shows that MPAA reduces social welfare while reducing bidding costs by 6.12%. Furthermore, with a 1.3% increase in average final satisfaction over conventional approaches, the TRAS algorithm achieves superior social welfare.

The remainder of this paper is organized as follows. Related work is reviewed in Section 2. The system model is formulated in Section 3. In Section 4, the design of the wireless resource auction algorithm is presented in detail. Simulation results and analysis are discussed in Section 5. Finally, conclusions are given in Section 6.

2. Related works

To solve the spectrum resource allocation problem, Alsharoa et al. [11] proposed a satellite–airborne–terrestrial network resource management scheme to maximize the system throughput through frequency division technique. Qin et al. [12] proposed a resource allocation mechanism for an air–ground integrated power IoT network, which effectively improves spectrum efficiency. Raveendran et al. [13] proposed a cyclic trilateral matching-based virtualized resource allocation mechanism for wireless networks, which improves user throughput and system resource allocation efficiency. Qin et al. [14] designed a content-oriented resource allocation algorithm and user-oriented resource allocation algorithm, which effectively improves the spectrum allocation efficiency of air–ground integrated networks. All of the above works use traditional methods, which make it more difficult to obtain complete information in the usual situation, thus making the traditional methods easy to converge to the local optimum. Some researchers have explored reinforcement learning [15].

Zhang et al. [16] proposed a fuzzy logic-assisted Q-learning model to intelligently and dynamically allocate resources using a centralized allocation model, which effectively improves the network throughput. Tian et al. [17] proposed a resource allocation framework based on multi-intelligence deep reinforcement learning, which effectively improves the quality of service in heterogeneous vehicle-mounted networks. Wanlu et al. [18] proposed a framework based on deep reinforcement learning and actor-critic technique, which effectively improves the convergence speed and spectrum reuse rate. Wang et al. [19] developed a multi-stack reinforcement learning (RL) algorithm, which can effectively reduce the resource allocation latency through the historical resource allocation scheme and user information. Since reinforcement learning requires a large amount of data to train the model and is more difficult to converge in complex environments, some researchers have used heuristics to solve the resource allocation problem [20]. Hu et al. [21] proposed a new heuristic learning method using deep reinforcement learning to accelerate the convergence of heuristics, which effectively reduces the delay of resource allocation and reduces the delay in the spectrum multiplexing rate. Torres et al. [22] propose a dual-objective hyper-heuristic algorithm for radio resource allocation to maximize the quality of user experience. Nguyen et al. [23] propose a meta-heuristic method to reduce the average user delay and increase the link transmission rate. Katwe et al. [24] based a meta-heuristic framework based on differential evolution, which jointly allocates the available resources among multiple users to effectively improve channel utilization. The above heuristics converge slowly in complex and large-scale problems.

Recently, due to its efficiency and fairness, the auction theory in the economic domain has been introduced into resource allocation algorithms. Zhang et al. [25] proposed a collaborative spectrum sharing scheme based on Vickrey-Clarke-Groves (VCG) auctions to effectively improve the spectrum utilization rate, which can be used for multi-unit auction. Su et al. [26] proposed a mechanism based on VCG auction which effectively improves the efficiency of the resource allocation scheme. Yadav et al. [27] propose a sealed-bid auction mechanism for spectrum allocation, which effectively improves spectrum utilization and reduces computational complexity. Single-tier auctions provide only a single auction phase, which leads to insufficient efficiency and accuracy in resource allocation. Zhu et al. [28] propose a blockchain-based two-phase secure spectrum smart sensing and sharing auction mechanism, which greatly improves the total utility and throughput of the system. Hosseinalipour et al. [29] propose a two-phase auction mechanism for cloud resources, which effectively improves the efficiency of cloud resource allocation. Zhang et al. [30] proposed auction-based multichannel collaborative spectrum allocation in hybrid satellite–terrestrial IoT networks to maximize the transmission rate through VCG auction and sequential Vickrey auction. The above schemes have insufficient consideration of the synergy and dynamic adjustment of resources in the auction process, and there are limitations in the efficiency and accuracy of solving the winner determination problem.

3. System model

The local power AIoT consists of the private edge cloud and various types of power terminals. The power private edge cloud is a cloud computing infrastructure that is close to the actual operational scene of the grid, providing low-latency, high-bandwidth data processing and analysis capabilities, and offering services such as load forecasting, equipment troubleshooting, distributed energy management, coordinated control of microgrids. As a hub for computing, storage, and network resources, the private edge cloud system assumes responsibility for status monitoring, power generation and consumption management, and provision of customized smart applications to promote advanced, green, and efficient energy use.
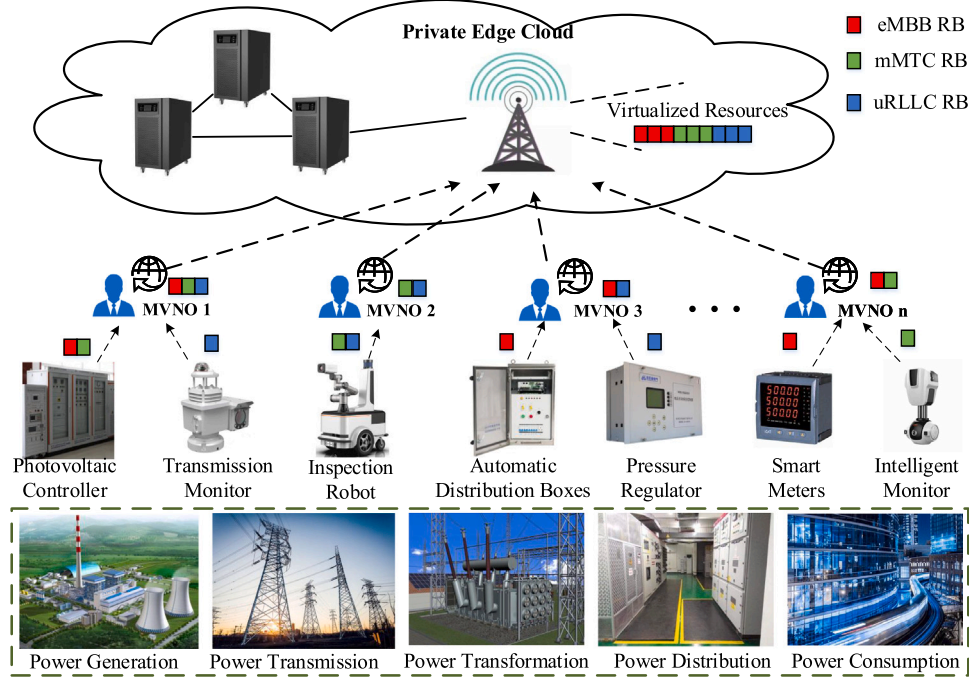
Fig. 1. A two-layer spectrum allocation architecture.

Photovoltaic controllers, inspection robots, smart meters, and other electricity terminals are used in the grid facility. These are responsible for collecting data on power equipment, executing control commands, and monitoring the status of the grid equipment at all times. They rapidly transmit the status updates they collect to the private edge cloud for immediate processing and take targeted action at any time based on instructions from the cloud, creating a seamless cycle of real-time response and management. To ensure real-time and reliable wirelessly transmission of data between the terminal and the private edge cloud, the two-layer spectrum allocation architecture is shown in Fig. 1.

MVNOs provide dedicated services for a specific slice or multiple slices of power terminals. However, MVNOs do not own or control any wireless network facilities and must purchase network access from MNOs to provide user services. To maximize the benefits of limited resources, we propose a multi-layer wireless resource allocation model that includes Power-Access Terminals, MVNO, and MNO. The terminal requests will be transmitted over three types of spectral slices, including eMBB (HP) slices, eMBB (LP) slices, and Massive Machine Type Communication(mMTC) slices. Among them, eMBB (HP) is a high-priority enhanced Mobile Broadband (eMBB) slice, eMBB (LP) is a low-priority eMBB slice, and the priority order among the three slices is eMBB (HP) > eMBB (LP) > mMTC.

The power terminals set is defined as k. When a terminal sends an access request to the MVNO, it provides the MVNO with slice type code, slice service type code parameters, and other primary information. Multiple MVNO form a MNO, which is defined as $MV_n, n \in N$. The MNO is the owner of the wireless resources and allocates the corresponding resources to each MVNO. Each power terminal obtains wireless slice resources from the accessed MVNO. We assumed that both the power terminal k and the MVNO remain unchanged during the resource allocation process. The MNO can provide available different types of wireless resources with slice labels $\{\alpha, \beta, \gamma, \ldots\} \in \mathcal{T}_y$. Each MVNO allocates radio resources under the corresponding slice for the accessed power terminals.

At a specific point in time, the MVNO gathers the current all power terminals' resource demands $\{\alpha_n, \beta_n, \gamma_n \ldots\}, n \in \mathcal{N}$. A wireless resource packet Ω_i denotes any combination of multiple wireless resource types,

e.g., mMTC and eMBB(HP) may constitute a wireless resource packet Ω_{me}. The MVNO can obtain a combination of resources instead of terminals. The maximum provisioning of all wireless resources $\mathcal{LI}(\mathcal{T}_y)$ is defined as the tolerance of $\mathcal{T}_y$, which is the set of all subsets of $\mathcal{T}_y$.

$$\mathcal{LI}(\mathcal{T}_y) = \left\{ \Omega_i | \Omega_i \subseteq \mathcal{T}_y^i, \forall \sum_{j=1}^{n} (\mathcal{T}_y^i)_j \leq \mathcal{H}_{\mathcal{T}_y}^i, i \in |\mathcal{T}_y| \right\} \quad (1)$$

where, $(\mathcal{T}_y^i)_j$ denotes the resource block demand of MVNO$_n$ for sliced resource block i. $\mathcal{H}_{\mathcal{T}_y}^i$ denotes the maximum number of resource blocks available for resource block i.

3.1. EMBB and mMTC transmission models

For an eMBB terminal, the data rate of terminal k at time slot t on Resource Block(RB) b can be expressed as $r_{kb}^e(t)$.

$$r_{kb}^e(t) = f_b log_2 \left(1 + \gamma_{n,k}^c \right) \quad (2)$$

$$\gamma_{n,k}^c = \frac{p_{kb}(t)h_{kb}(t)}{\sigma^2} \quad (3)$$

where f_b is the transition bandwidth of RB b. $\gamma_{n,k}^c$ is the channel gain between terminal k and MNO. $h_{kb}(t)$ is the transmitted time-varying Rayleigh fading channel gain, $p_{kb}(t)$ is the downlink transmission power allocated to terminal k at time slot t.

Therefore, the data rate of eMBB terminal k overall allocated RBs $r_k^e(t)$ can be calculated using Eq. (4).

$$r_k^e(t) = \sum_{b \in B} x_k^e(t) r_{kb}^e(t) \quad (4)$$

$$x_k^e(t) = \begin{cases} 1, & \text{if the RB } b \text{ is allocated to eMBB user } k \text{ at time } t \\ 0, & \text{otherwise} \end{cases} \quad (5)$$

where $x_{kb}^e(t)$ is the eMBB terminal's RB scheduling indicator code at time slot t. Assumed each mMTC terminal needs only one RB, the data rate of an mMTC terminal can be expressed as $r_k^m(t)$ due to the small amount of mMTC sliced data.

$$r_k^m(t) = x_k^m(t) f_b \log_2 \left(1 + \frac{p_{kb}(t) h_{kb}(t)}{\sigma^2} \right) \quad (6)$$

$$x_k^m(t) = \begin{cases} 1, & \text{if the RB } b \text{ is allocated to mMTC user } k \text{ at time } t \\ 0, & \text{otherwise} \end{cases} \quad (7)$$

where $x_k^m(t)$ is the mMTC terminal's RB scheduling indicator code at time slot t.

3.2. Problem formulation

To meet the service needs of users, we use terminal satisfaction to characterize the transmission service quality of each power terminal. The satisfaction function S_{at} is detailed in Eq. (8).

$$S_{at} = \begin{cases} 0.5, & |R_{ind}| = 0 \\ \dfrac{1}{1+e^{-\frac{|R_{ind}|}{R_{req}-|R_{ind}|}}}, & |R_{ind}| = 1, 2, \ldots, (R_{req}-1) \\ 1, & |R_{ind}| = R_{req} \end{cases} \quad (8)$$

where, $R_{ind} = \{1, \ldots, RB_n\}$ denotes the set of resource requirements of terminals. It is assumed that the maximum number of RB that each terminal can get is not more than R_req, i.e., the maximum satisfaction level of the power terminal is 1. The actual number of RB that can be obtained is $|R_{ind}|$, and the minimum satisfaction level of power terminals is 0.5. Considering that there is a difference in the priority level of the individual slices, the weighting coefficients of the eMBB(HP), eMBB(LP), and mMTC slices are defined as ω_{eH}, ω_{eL}, and ω_{em} respectively. Therefore, the weighted terminal satisfaction of any terminal within the eMBB(HP) slice is $\omega_{eH}S_{at}^h$. Similarly, it is $\omega_{eL}S_{at}^l$ for eMBB(LP), and $\omega_{em}S_{at}^m$ for mMTC. Hence, the average weighted terminal satisfaction $\overline{S_{at}}$ can be calculated using Eq. (9).

$$\overline{S_{at}} = \frac{\sum_{h=0}^{H} \omega_{eH}S_{at}^h + \sum_{l=0}^{L} \omega_{eL}S_{at}^l + \sum_{m=0}^{M} \omega_{em}S_{at}^m}{k} \quad (9)$$

Meanwhile, to minimize the MVNO's cost in acquiring RB from MNO, it is considered a metric for objective optimization. It is defined as $U_n(R) = \omega_i p_i$, where p_i represents the MVNO's final bid for the resource package combination Ω_i, and ω_i is the weighting coefficient. The MVNO's cost is determined by the final price it pays, with lower prices resulting in greater benefits.

$$P0: \quad \underset{\overline{x_{k,n}}, \overline{x_k^e}, \overline{x_k^m}}{max} \; \overline{S_{at}}\omega_{at} + \sum_{n \in N} \frac{1}{U_n(R)}$$

$$\text{s.t.} \quad \sum_{n \in \mathcal{N}} x_{k,n} \leq 1, \forall k \in \mathcal{K} \quad (9(a))$$

$$\sum_{n \in \mathcal{N}1Az} x_{k,n}\mathcal{D}_{MV}^n \leq \mathcal{T}_y, \forall k, n \quad (9(b))$$

$$\sum_{n \in \mathcal{N}} x_{k,n}\alpha_n \leq \mathcal{H}_{\mathcal{T}_y}^\alpha \quad (9(c))$$

$$\sum_{n \in \mathcal{N}} x_{k,n}\beta_n \leq \mathcal{H}_{\mathcal{J}_y}^\beta \quad (9(d))$$

$$\qquad\qquad\qquad\qquad\qquad (10)$$

$$\sum_{n \in \mathcal{N}} x_{k,n}\gamma_n \leq \mathcal{H}_{\mathcal{J}_y}^\gamma \quad (9(e))$$

$$\sum_{n \in \mathcal{N}} x_{k,n}r_k^e(t) \geq d_k^e, \forall k, n \quad (9(f))$$

$$\sum_{n \in \mathcal{N}} x_{k,n}r_k^m(t) \geq d_k^m, \forall k, n \quad (9(g))$$

$$\sum_{n \in \mathcal{N}} x_{k,n}b_n \geq P_f, \forall n \in \mathcal{N} \quad (9(h))$$

$$x_{k,n} \in \{0,1\}, \forall k, n \quad (9(i))$$

where, 9(a) indicates that each terminal k can be associated with at most one MVNO. 9(b) indicates that the number of slice types that MVNO$_n$ obtains from the MNO cannot be greater than $\mathcal{T}_y$. 9(c), 9(d), and 9(e) state that the total number of sliced RBs obtained by MVNO$_n$ from MNO cannot exceed the maximum number of RB's provided by MNO. 9(f) and 9(g) indicate that the RBs allocated by MVNO to the terminals meet the communication requirements of eMBB and mMTC

terminals, respectively. 9(h) indicates that the MVNO offer must be at least greater than or equal to the predetermined price of the MNO. 9(i) indicates that the variable $x_{k,n}$ is a binary variable. It is assumed that each terminal k submits only one kind of sliced resource request and all the smallest RBs are labeled with different counting symbols by the MVNO.

The optimization problem $P0$ consists of both discrete and continuous variables, hence it is considered as a Mixed Integer Nonlinear Programming (MINLP) problem and can thus be proved to be a standard traveler problem. To solve the NP-hard problem, we design a hierarchical auction model across terminals, MVNOs, and MNOs. The upper layer auction solves the problem of MVNO resource acquisition, while the lower layer auction solves the problem of power terminal resource allocation.

4. Wireless resource auction algorithm

In this paper, we propose a Multi-hop Progressive Auction Algorithm (MPAA) with MVNOs and MNOs. To solve the resource allocation problem of MVNO and power terminals, a Terminal Resource Allocation Strategy (TRAS) based on utility optimization is proposed.

4.1. Multi-hop progressive auction algorithm

In MPAA, each buyer designs a unique bidding strategy, using open bidding to form hybrid bids. The sliced resource valuation is updated through comparisons with existing hybrid bids, enhancing cost-effective resource allocation. This auction must satisfy the following conditions: (a) The information about all bidders' bids is transparent and each bidder has access to information about other bids. (b) Completing the auction within the specified time. (c) Avoid jump bidding and mitigate threshold issues.

4.1.1. Primitive pricing and bidding resource portfolio

The MNO possesses the time–frequency resources in a particular band, and a cost is associated with reserving these resources. The cost is composed of a resource block's reservation cost P_{rev} and a slice instantiation cost P_{init}. The MNO's minimum reservation price is $P'_{rev} = P_{rev} + P_{init}$. As terminals have diverse transmission quality requirements, the MNO will preferentially reserve channel resources for high-priority slices.

4.1.2. MVNO bidding resource portfolio

To simplify the portfolio of MVNO bidding resources, we have defined the following concepts.

Resource Block: A resource block is the smallest unit of resource type that cannot be divided, denoted as $\{\alpha, \beta, \gamma, \ldots\}$. It can be used to represent a variety of wireless resources, such as eMBB resource blocks, uRLLC resource blocks, and mMTC resource blocks.

Resource Package: Different wireless resources are assembled into a resource package, denoted as $\{\Omega_1, \Omega_2, \ldots\}$. A resource package consists of squares of different resources.

Resource grouping: A resource grouping consists of resource packages of different resource types, indicated as $\{\Phi_1, \Phi_2, \ldots\}$. Resource grouping ϕ_i consists of different combinations of Ω_i, where there are no duplicate resource types between Ω_i.

To describe the resource portfolio and its value, at this stage, we define a uniform bidding language as follows.

$$b_n^i = \; <n, \Omega_i, v_n(\Omega_i)> \quad (11)$$

where, n is the nth MVNO, Ω_i is the ith resource portfolio, and $v_n(\Omega_i)$ is the MVNO's evaluation value for resource portfolio Ω_i. $\Phi_1, \Phi_2, \ldots, \Phi_i \in \mathcal{T}_y$ is a collection of what are known as resource grouping.

$$\bigcup_{i=1}^{r} \Phi_i = \mathcal{T}_y, \Phi_i \cap \Phi_j = \emptyset, \forall i \neq j \quad (12)$$

The definition indicates that each resource package in the set of resource packages collectively constitutes a complete set of resource types $|\mathcal{T}_y|$, and that there are no overlapping sliced resource types between any of the resource packages. For instance, a hybrid bid B comprises the set $\Gamma_i = \{\Phi_1, \Phi_2, \ldots, \Phi_r\}$, denoted $E(\Gamma_i); v(\Phi_1), v(\Phi_2), \ldots, v(\Phi_n)$.

Therefore, a hybrid bid comprises $3n+1$ pieces of information. The initial piece of information is the total valuation of the hybrid bid c. The remaining $3n$ pieces of information are: (1) The description of the resource package block Φ_i. (2) The value of the bids on resource package block Φ_i. (3) the bidder identity of resource package block Φ_i. We use the following expression to represent a composite bid.

$$B = <n, \Gamma_i, E(\Gamma_i)> \tag{13}$$

Each MVNO is tasked with solving its bid composition problem. They are provided with a hybrid bid request that includes non-overlapping resource packages. We maximize an objective function based on their preferences. This problem is shown as $P1$.

$$P1: \max \quad U(v_n(\Omega_i)x_n^i),$$
$$\text{s.t.} \quad \Omega_i \cap \Omega_j = \varnothing, i \neq j \tag{14}$$
$$x_n^j \in \{0, 1\}, \forall b_n^i \in Y_n^g$$

where $\Omega_i \cap \Omega_j = \varnothing$ indicates a resource type that is not duplicated between resource packages. x_n^j is a binary decision variable. If $\forall b_n^i \in Y_n^g$ is assigned to terminal MV_n, $x_n^j = 1$. Otherwise, $x_n^j = 0$. Where Y_n^g is the set stored by MV_n in gth round, which contains all mixed bids previously made by other MVNOs that have no more than g kinds of each resource package in the mixed bids. The gth round is the auction of rounds in the current auction, and when gth round is reached, the maximum number of kinds of each resource grouping in the mixed bids must not exceed the gth rounds. The set Y_n^g contains the candidate bids that can be used to form a new mixed bid.

$$Y_n^g = C_n^g \cup \{b_n^i, \forall \Omega_i \subseteq \mathcal{T}_y, |\Omega_i| \leq g\} \tag{15}$$

$$C_n^g = C_n^{g-1} \cup \left(\bigcup_{m \in N, m \neq n} B_m^{g-1}\right) \cup C_n^0 = \varnothing \tag{16}$$

4.1.3. MPAA details

To solve problem $P1$, we propose a Multi-hop progressive auction algorithm. When $g = 1$, each MVNO bids for only one resource and broadcasts its bid. Each MVNO compares its own bid with the bids of other MVNOs and stores the highest value in its respective repository CB_0. If there are multiple identical bids for a resource, the number of multiple winners q^K is broadcast among the bidders before the end of phase 1. The pseudo-code of the algorithm is as follows.

Algorithm 1: Stage-One Adaptive Resource Allocating Algorithm

---
Input: $COM_i, |T|$
Output: SD^1
1: **for** $i = 1 : |T|$ **do**
2:   **if** $|\Omega_i| = 1$ **then**
3:     **if** $v_n(\Omega_i) > v_m(\Omega_i), \forall m \neq n \in N$ **then**
4:       $SD^1 \longleftarrow b_n^i$
5:     **end if**
6:   **end if**
7:   **if** $|\Omega_i| \geq 2$ **then**
8:     Select winners q^K, Select $|\Omega_i|$ in SD^1
9:     $|\Omega_i| \longleftarrow \frac{|\Omega_i|}{q^K}$
10:     Update SD^1
11:   **end if**
12: **end for**
13: Return SD^1

If $g > 1$, each MVNO constructs hybrid bids by combining bids, and total valuation of the new hybrid bids must be greater than the current best hybrid bid. If no new hybrid bids are proposed in the

gth round of auction, the auction jumps to the next round. During the auction at each round, the bid for the combination of its own demand resource types is gradually increased until the valuation of a resource package in the current mixed bid does not increase. When $g = |\mathcal{T}_y|$, each MVNO stops proposing new hybrid bids. The hybrid bids are stored in their respective evaluation repositories SD^g, updating their respective selected resource packages as described in **Algorithm 2**. According to the analysis derived from the pseudocodes of **Algorithm 1** and **Algorithm 2**, the time complexity of the MPAA is $O(n^2)$.

Algorithm 2: Multi-hop Auction Algorithm

Input: b_n^i, SD^1
Output: $SD^{|S|}$
1: **for** $g = 2 : |S|$ **do**
2:   **while** $E(P_n) - E(P_m) \leq v_n(\Omega_i)$ **do**
3:     **if** $\Omega_i \cap \Omega_j = \varnothing, i \neq j$ **then**
4:       $\Phi \longleftarrow \Omega^i$
5:       $P_n \longleftarrow \{\Phi_1, \Phi_2, \ldots, \Phi_{|C^g|}\}$
6:       $E(P_n) = \sum_{i=1}^{|C^g|} p_n(\Phi_i)$
7:     **end if**
8:     **if** $E(P_n) > E(P_m)$ **then**
9:       $SD^g \longleftarrow B_n^g(E(P_n))$
10:     **else**
11:       $E'(P_n) = E(P_n) + \epsilon$
12:       $SD^g \longleftarrow B_n^g(E'(P_n))$
13:     **end if**
14:   **end while**
15:   $SD^g \longleftarrow B_n^g$
16:   $C^g \longleftarrow C^g \cup \bigcup_{n \in N, n \neq m} B_m^g$
17: **end for**
18: Return SD^S

4.2. Terminal resource allocation strategy based on improved particle swarm optimization

Since each wireless resource block is an independent individual, multiple terminals competing for the same resource block can only have one winner. When the number of competing terminals is large, the computational complexity of the spectrum allocation algorithm is high. To solve the resource allocation problem of MVNO and power terminals, the TRAS based on Improved Particle Swarm Optimization is proposed. The algorithm contains two parts: Probabilistic Solution Correction Algorithm (PSCA) and Improved Discrete PSO.

4.2.1. Terminal bid initialization and problem modeling

In the terminal resource allocation process, the auctioneer is the MVNO, and the bidder is the power terminal K. The number of resource blocks obtained by power terminal K will affect its satisfaction. We define the terminal's bid v_k^i for a resource block as follows.

$$v_k^i = p_b R_b \omega_c \mu \tag{17}$$

where R_b is the number of resource blocks included in the bid submitted by terminal K. ω_c is the valuation factor, which increases with the increase of R_b. It is defined as $\omega_c = R_b / R_{req}$. μ is a random evaluation factor, $\mu \in [1, 1+\tau]$, where τ is a small positive value. p_b is the base selling price of sliced resources to the MVNO.

$$p_b = \begin{cases} p_b^{eH}, & \text{eMBB(HP)} \\ p_b^{eL}, & \text{eMBB (LP)} \\ p_b^m, & \text{mMTC} \end{cases} \tag{18}$$

The bid of each terminal is defined as follows.

$$b_k^i = \langle n_k, R_{ind}, v_k^k \rangle \tag{19}$$

where, n_k is the terminal number, R_{ind} is the resource demand set of the terminal, and v_k^i is the bid for the corresponding resource combination.

The bid set $B_k = \{b_k^1, b_k^2, \ldots, b_k^i\}$. The resource allocation problem $P2$ between the MVNO and power terminals can be formulated as follows.

$$P2 : \max \quad U\left(v_k^i, x_n^i\right), x_n^i \in \{0, 1\} \tag{20}$$
$$\text{s.t.} \quad b_k^i \cap b_k^j = \varnothing, i \neq j$$

The constraint $b_k^i \cap b_k^j = \varnothing$ indicates that the two winning resource combinations do not overlap. x_n^i is a binary decision variable, where $n \in N$. If the resource combination R_{ind} is allocated to terminal k, $x_n^i = 1$; otherwise, it is 0. It is demonstrated that the $P2$ problem is a winner problem for multi-objective optimization.

The number of bids proposed by terminals is very large, leading to relatively low efficiency in solving the $P2$ problem. For example, assuming that a certain power terminal requires a certain number of resource blocks $R_{req} = 5$, and the MVNO can provide 100 sliced resource blocks. According to the analysis, the maximum number of effective bids b_{max} proposed by this terminal is as follows.

When $R_{req} = 5$, the effective value of R_b are 1,2,3,4,5.
(1) If $R_b = 1$, the number of effective bids is 100.
(2) If $R_b = 2$, the number of effective bids is C_{100}^2.
(3) If $R_b = 3$, the number of effective bids is C_{100}^3.
(4) If $R_b = 4$, the number of effective bids is C_{100}^4.
(5) If $R_b = 5$, the number of effective bids is C_{100}^5.
So, $b_{\max} = 100 + C_{100}^2 + C_{100}^3 + C_{100}^4 + C_{100}^5 = 79375495$.
This is the number of effective bids proposed by a single terminal. In this paper, the following strategy is adopted to screen all bids.

(1) Each power terminal K initializes its bid b_k based on its own maximum required resource block number R_{req}.

(2) If $R_b = 1$, choose the maximum bid b_k^1 for the resource block valuation v_k^i. Determine whether a bid is required for $R_b = 2$. If so, continue with the previous section. If it is not required, then continue to judge the next value R_b.

(3) Until $R_b = R_{req}$, pick the bid $b_k^{R_{req}}$ that maximizes the resource block valuation $v_k^{R_{req}}$.

(4) The number of screened bids $b\left(N_k\right)$ for each power terminal K is as follows.

$$b\left(N_k\right) = j, j \in N^+, j \leq R_b \tag{21}$$

4.2.2. Discrete particle swarm optimization

Particle Swarm Optimization (PSO) is an algorithm evolved from swarm search and has been widely applied to various optimization problems. The position and velocity of each particle can be updated using the following equations.

$$v_i^{t+1} = \omega v_i^t + c_1 r_1 (p_i^t - x_i^t) + c_2 r_2 (g^t - x_i^t),$$
$$i = 1, 2, \ldots, S; t = 1, 2, \ldots, U \tag{22}$$

$$x_i^{t+1} = x_i^t + v_i^{t+1},$$
$$i = 1, 2, \ldots, S; t = 1, 2, \ldots, U \tag{23}$$

where v_i^{t+1} is the velocity, x_i^{t+1} is the position. S represents the number of particles; U is the maximum number of iterations; ω is the inertia weight parameter; c_1 and c_2 are learning factors that control the positive knowledge of individual and population historical optimal positions in each iteration. r_1 and r_2 are two random numbers in the range of $[0, 1]$; p_i^t and g^t are the individual and population historical optimal positions.

In this article, we use the particle swarm optimization algorithm to solve the winner's objective function $P2$ in the bidding problem. The fitness function Fit_i^t is defined as follows:

$$Fit_i^t = \sum_{i=1}^{|B_k|} \overrightarrow{X_i^t} \times v_k^i\left(R_b\right) \tag{24}$$

where, $\overrightarrow{X_i^t}$ represents a discretized particle position vector, where each component of the vector satisfies $X_i^t \in \{0, 1\}$. When $X_i^t = 1$, the corresponding bid B_k is selected. When the fitness function value is larger, it means that the currently selected feasible bid solution vector is more appropriate.

The initial positions x_i^t and updated velocities v_i^t of the particle swarm algorithm are continuous functions, it is evident that X_i^t cannot be directly obtained from x_i^t. Therefore, the following definitions are introduced.

Definition 1. Since the solution vector of the $P2$ problem is a discrete vector value, we discretize the continuous position x_i^t in the particle swarm algorithm. Suppose x_i^t is the current continuous value of the particle position variable, $\delta(x_i^t)$ is the discretized value of the position variable, and $\delta(x_i^t) \in \{0, 1\}$. Subsequently, the probability value of $\delta(x_i^t) = 1$ is defined as $p(x_i^t)$. Since the discretization of continuous values needs to satisfy symmetry, $p(x_i^t)$ should satisfy the properties as follows.

(1) When x tends to $-\infty$, $p(x_i^t)$ tends to 0: $\lim\limits_{x \to -\infty} p(x_i^t) = 0$
(2) When x tends to $+\infty$, $p(x_i^t)$ tends to 1: $\lim\limits_{x \to +\infty} p(x_i^t) = 1$
(3) When x tends to 0, $p(x_i^t)$ tends to steady state: $\lim\limits_{x \to 0} p(x_i^t) = \frac{1}{2}$
(4) Larger values of $p(x_i^t)$ tends to convert to 1: $p'(x_i^t) \geq 0$
(5) Symmetry requirements: $p(x_i^t) + p(-x_i^t) = 1$
The discrete state transition function can be expressed as:

$$p(x_i^t) = \frac{1}{1 + e^{-x_i^t}} \tag{25}$$

If $\mu > p(x_i^t)$, then $\delta(x_i^t) = 1$; conversely, $\delta(x_i^t) = 0$, where μ is the mean of the $[0, 1)$ distribution. Finally, the discretized position vector is $\overrightarrow{X_i^t} = \left\{\delta_1\left(x_i^t\right), \delta_2\left(x_i^t\right), \ldots, \delta_S\left(x_i^t\right)\right\}$.

4.2.3. Probabilistic solution correction algorithm

The above discretization process, $\overrightarrow{X_i^t}$ has strong randomness. This strong randomness has a high probability of leading to the loss of terminal bids with higher offers. In this section, the PSCA algorithm is proposed to correct the discrete position vector $\overrightarrow{X_i^t}$. Correcting the discrete position vector $\overrightarrow{X_i^t}$ requires constructing a feasible potential bid vector solution $\overrightarrow{P_o}$ with each component $P_o \in \{0, 1\}$.

Assume that the power terminal K has proposed a total of m valid bidding schemes to compete for the wireless slice resource block. Construct an $m \times m$ square matrix based on these m bids, which is expressed as M_{cf}.

$$M_{cf} = \begin{bmatrix} C_1^1 & C_1^2 & & C_1^{m-1} & C_1^m \\ C_2^1 & C_2^2 & & C_2^{m-1} & C_2^m \\ & \vdots & \ddots & & \vdots \\ C_{m-1}^1 & C_{m-1}^2 & & C_{m-1}^{m-1} & C_{m-1}^m \\ C_m^1 & C_m^2 & & C_m^{m-1} & C_m^m \end{bmatrix} \tag{26}$$

where, C_m^m is a binary number, $C_m^m \in \{0, 1\}$, expresses whether there is a conflict between two bids, i.e. whether there is a conflict between the bid $b_i^{R_b}$ of terminal i and the bid $b_j^{R_b}$ of terminal j for the same resource block. If there is a conflict, $C_m^m = 1$, and vice versa is 0. M_{cf} is a conflict judgment matrix, through which conflict bids can be quickly judged, and its conflict judgment process is shown in Fig. 2.

Suppose $\overrightarrow{P_{in}}$ is a preliminary solution vector, which may conflict with bids whose components are already set to 1. We transform it into a potential solution vector $\overrightarrow{P_o}$. To avoid the bids b_k^i of potential solutions from being discarded due to low valuation, this paper uses random chance comparison to construct a more enlightening potential solution vector in the process of comparing the size of bid valuation.

Definition 2. In the process of comparing the size of the bid valuation of a sequence L, if there exists $\forall i \neq j$, satisfying $l_j \geq l_i$, then there exists a σ $(0 < \sigma < 1)$ probability to give the decision $l_j \geq l_i$ and a $1 - \sigma$ probability to give the decision that $l_j < l_i$.

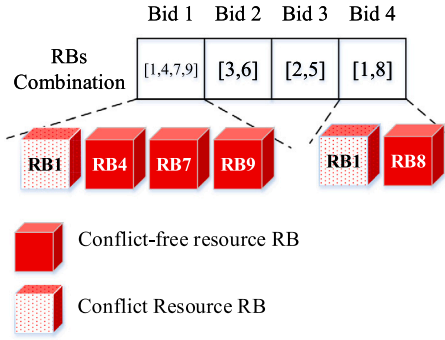**Fig. 2.** Bid Conflict.

We take this potential bid feasible solution $\vec{P_o}$ as the modified solution of the discrete position vector $\vec{X_i^t}$, defined as $\vec{X_i^{t*}}$. The detailed construction process is as described in **Algorithm 3**.

Algorithm 3: Probabilistic Solution Correction Algorithm (PSCA)

Input: b_k^i, M_{cf}, σ
Output: X_i^{t*}
1: Initialize L, H, σ
2: **for** $i = 1 : |B_k|$ **do**
3:   **for** $n = 1 : |B_k|$ **do**
4:     **if** $b_k^n > b_k^i$, $i \neq n$ **then**
5:       **if** $\sigma > $ rand $(0, 1)$ **then**
6:         b_k^n insert L
7:       **else**
8:         b_k^i insert L
9:       **end if**
10:     **end if**
11:   **end for**
12: **end for**
13: $H = L$
14: **if** $L \neq \oslash$ **then**
15:   **for** $m = 1 : |H|$ **do**
16:     **for** $j = 1 : |L|$ **do**
17:       **if** $m \neq j$, H_m conflict with L_j **then**
18:         Remove H_m from H
19:       **end if**
20:     **end for**
21:   **end for**
22: **end if**
23: Compare and correct H with the conflict matrix M_{cf}
24: Return X_i^{t*}

4.2.4. Improved discrete PSO algorithm

Through the work in the previous section, we obtain the modified discrete position vector $\vec{X_i^{t*}}$. In this section, the TRAS algorithm is proposed to update the global optimal solution g^t of the particle swarm optimization algorithm. the TRAS algorithm introduces the Simulated Annealing (SA) algorithm, which overcomes the problem of deterioration of the population diversity during iteration. TRAS algorithm avoids falling into the local optimal solution. We introduce the following parameter p:

$$p = exp \frac{-Fit(g^{t+1}) - Fit(g^t)}{T^t} \qquad (27)$$

The parameter p indicates the probability that the suboptimal solution is accepted. When p is too large, the convergence of the algorithm is poor. When p is too small, the algorithm is inefficient and easily falls into the local optimal solution. Where T is the temperature of the current system. If T is too large, it will cause the probability p to

converge to 1, which means that the algorithm will accept suboptimal solutions with higher probabilities. Update $T^{t+1} = r \times T^t$, r is the parameter that controls the rate of temperature change in $[0, 1]$. If r is too large, the probability of finding a globally optimal solution using the algorithm will be higher, but this will be a very time-consuming process. Conversely, if r is too small, the search process will be faster and the algorithm may fall into local convergence. Therefore, r is updated using a linearly decreasing method with population iterations, as shown in the following equation:

$$r = \frac{U - t}{U} \qquad (28)$$

where U is the maximum number of iterations and t is the current number of iterations. As the population continues to evolve, the diversity of the population decreases and the similarity of the particles increases. To avoid falling into the optimal solution, the suboptimal solution p_n^t is defined to be the nth particle in the tth iteration and n is a random number located between 0 and t. Because n is too small, it is difficult to jump out of the local optimal solution in the late iteration. However, when n is too large, the particles oscillate severely and it is difficult to converge in the early iteration. The specific algorithmic process is described as **Algorithm 4**. According to the analysis derived from the pseudocodes of **Algorithm 3** and **Algorithm 4**, the time complexity of the TRAS algorithm is $O(n^2)$.

Algorithm 4: Improved Discrete PSO

Input: b_k^i, x_i^t, v_i^t, p_i^t, g^t
Output: S_{ol}
1: Initialization: Dimension $D = |B_k|$, x_i^t, v_i^t, p_i^t, g^t
2: **while** $t \leq U$ **do**
3:   **for** $i = 1 : S$ **do**
4:     Update v_i^t by Eq. (22)
5:     Update x_i^t by Eq. (23)
6:     Discrete x_i^t to get $\vec{X_i^t}$ by Eq. (25)
7:     Calculate the fitness value Fit_i^t of the particle $\vec{X_i^t}$ in PSCA Algorithm
8:     **if** $Fit_i^t(x_i^t) > Fit_i^t(p_i^t)$ **then**
9:       $p_i^t = x_i^t$
10:     **end if**
11:   **end for**
12:   **if** $Fit(g_{temp}^{t+1}) > Fit(g^t)$ **then**
13:     **if** $p > $rand$(0, 1)$ **then**
14:       Update the global optimal solution, $g^{t+1} = p_n^t$;
15:     **else**
16:       $g^{t+1} = g^t$
17:     **end if**
18:   **else**
19:     $g^{t+1} = g_{temp}^{t+1}$
20:   **end if**
21: **end while**
22: Return S_{ol}

---

5. Simulation results

5.1. Simulation parameter and performance metrics

In this section, we set the parameters of MPAA and TRAS to simulate the experiments. All experiments were performed using MATLAB R2021b on a PC with an Intel Core i5 (3 GHz) and 32 GB of RAM. The simulation parameters are shown in Table 1.

We employ four evaluation metrics for evaluated-different performance attributes of the algorithm.

(1) Social Welfare SW: the sum of the gains from all auction participants;

$$SW = \omega_{sell} \left(v_n(\Omega_i) - P_f(\Omega_i) \right) + \omega_{buy} \left(P_n(\Omega_i) - v_n(\Omega_i) \right) \qquad (29)$$

Table 1
Simulation parameters.

Algorithm	Parameters	Values
MPAA	Number of MVNOs	3~11
	Cost per auction round	2 ms
	Number of MNO resource blocks	100
	Number of slice types	3,4,5,6,7
	bid valuation increment ϵ	1,5,10,15
	Cost of MNO reserved RBs	2
TRAS	Nonlinear exponent ω	3
	Positional quantities x	[−100,100]
	Speed v	[−200,200]
	Topological structure	toroidal
	Population size	53
	Initial temperature T_0	100
	End temperature T_f	0.1

Fig. 3. The change in social welfare as the number of rounds increases.

Fig. 4. MPAA Bidding Progress.

where, $P_f(\Omega_i)$ is the slicing cost of the MNO. $v_n(\Omega_i)$ is the bidding price of the MVNO. $P_n(\Omega_i)$ is the bidding budget of the MVNO. ω_{sell} and ω_{buy} are the auctioneer's revenue weight and the bidder's revenue weight, respectively.

(2) MVNO Cost $U_n(R)$: The cost of the MVNO participation in auction bidding;

(3) Superiority Rate S_{up}: the quotient of the current fitness value and the optimal value of the problem;

$$S_{up} = \frac{g^t}{g^{max}} \tag{30}$$

where g^t is the current adapted value of the algorithm. g^{max} is the optimal value of the objective problem.

(4) Terminal Satisfaction S_{at}: an indicator that measures the matching of bid allocations to the needs of terminals.

5.2. Simulation result analysis of MPAA

In the simulation experiments of MPAA, we analyze the effect of different numbers of MVNOs and bid valuation increments ϵ on the performance of MPAA. And we compare the MPAA with three different algorithms [31–33].

5.2.1. The effect of bid evaluation increments on social welfare and convergence time

Fig. 3 shows the change in the social welfare of the MPAA as the number of rounds increases with different bid valuation increments ϵ. As can be seen in the figure, the social welfare first increases rapidly and then stops varying after reaching the inflection point. It can be observed that the larger the bid valuation increment ϵ, the smaller the social welfare. However, the larger the bid valuation increment ϵ, the faster the convergence rate. This is because the increase of bid valuation increment ϵ causes MVNOs to exit the auction early due to bidding over budget. This may result in the final bidding of the MVNO being well below the budgeted threshold, which reduces social welfare. The increase in bid valuation increment ϵ also reduces the number of auction rounds, which decreases the convergence time of MPAA.

5.2.2. MPAA bidding progress

Fig. 4 shows the bidding progress for four different types of slicing resources. It can be seen that the value of slice resources varies considerably between rounds, but the total value increases gradually based on the bid valuation increment ϵ. The figure shows that some slice resources did not generate bids in some rounds. This is because, during the auction process, the MVNO discovered that other bidders were bidding too high for the slice resources. To reduce the unnecessary bidding cost, MVNO shifted the budget of that slice resource to others.
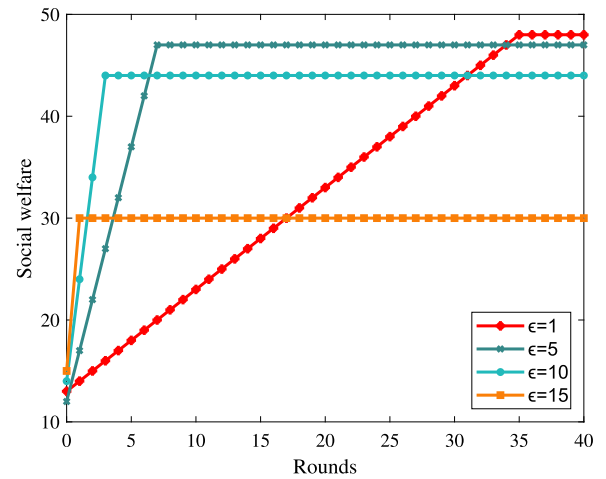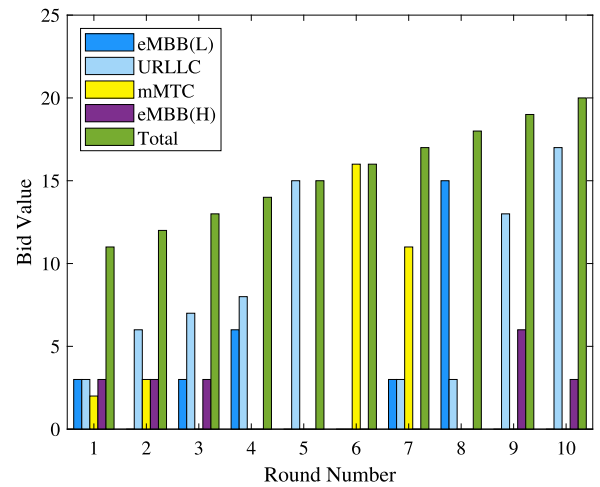
5.2.3. Effect of bid valuation increments on auction consumption delay

Fig. 5 illustrates the effect of the number of MVNOs on the auction consumption delay of MPAA. As shown in the figure, the auction consumption delay increases with the increase in the number of MVNOs. This is because the complexity of the auction rises as the number of MVNOs increases. When the number of MVNOs holds constant, the delay decreases as the bid valuation increment ϵ increases. This is because the entire auction is completed in a short time when ϵ is increased, which reduces the auction consumption latency of MVNO.

5.2.4. Comparison of social welfare and MVNO costs

The social welfare of the four algorithms with different numbers of MVNOs is shown in Fig. 6(a). As seen in the figure, the social welfare of the centralized algorithm is the highest. The social welfare of MPAA is not much different from that of centralized algorithm [31]. The social welfare of the randomized algorithm [32] is the lowest. This is because resource bids in MPAA are determined by several rounds of auctions, which avoids revenue depletion caused by single bids and increases the social welfare of MPAA. Fig. 6(b) compares the MVNO cost of MPAA and the Central algorithm. The figure shows that MVNO cost of MPAA saves 6.12% compared to the Central algorithm. This is because MVNOs in MPAA bid rationally in auctions, which can reduce unnecessary costs and increase MVNO revenue.
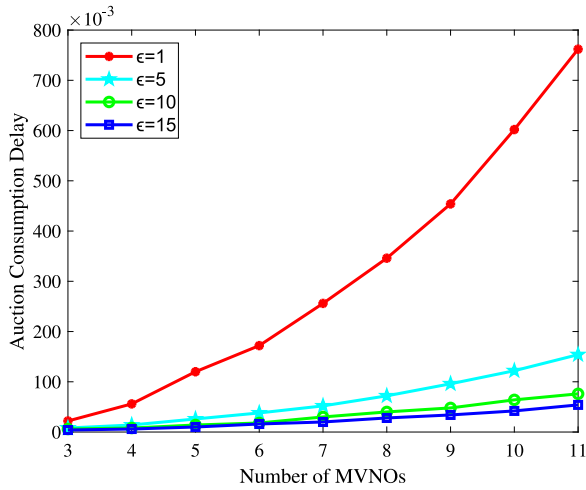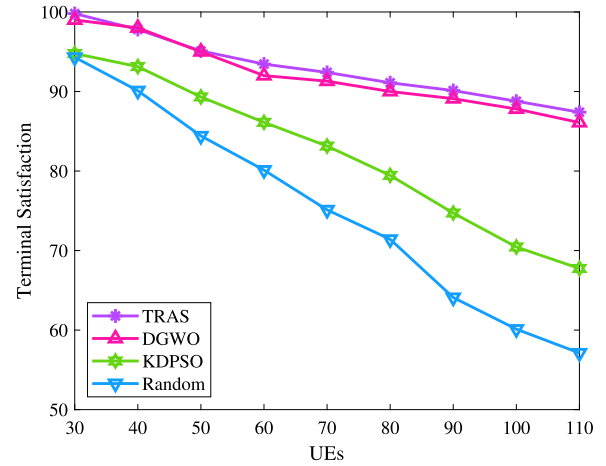
Fig. 5. Variation in auction consumption delay.
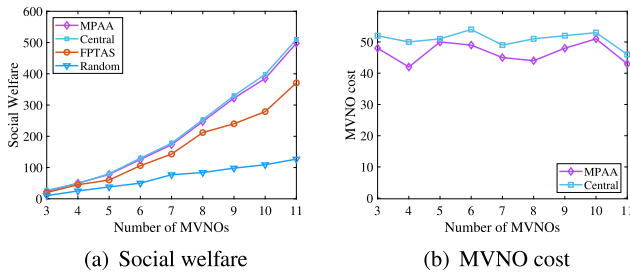

Fig. 6. Comparison of social welfare and MVNO cost for different algorithms.
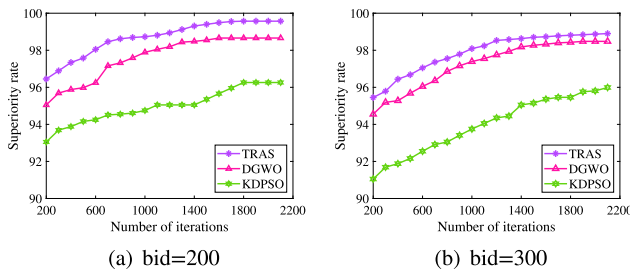

Fig. 7. Superiority Rate for different algorithms.

5.3. Simulation result analysis of the TRAS

5.3.1. Superiority rate

In Fig. 7, we compare the average superiority rates of the three algorithms [32,34,35]. Fig. 7(a) and Fig. 7(b) show the superiority rates for two different bid totals. The figure shows that the superiority rate increases gradually as the numbers of iterations increase. Compared to other algorithms, TRAS has the largest superiority rate. This is because the PSCA algorithm is used to correct the discretized error, which makes the solution closer to the optimal solution, thus increasing the superiority rate.

5.3.2. Terminal satisfaction

Fig. 8 illustrates the average terminal satisfaction for the four algorithms. As the number of terminals increases, the average terminal satisfaction gradually decreases. TRAS has the highest terminal satisfaction. DGWO [34] has terminal satisfaction closer to TRAS. KDPSO [35] and Random algorithm have lower terminal satisfaction. This is because

Fig. 8. The TRAS bidding progress.

KDPSO is prone to fall into local optimization, which leads to a decrease in terminal satisfaction. The TRAS adopts a simulated annealing algorithm to optimize the global search, which effectively avoids the local optimum problem and improves terminal satisfaction. In addition, the PSCA algorithm is used to correct the discretized error in TRAS, resulting in higher terminal satisfaction than DWGO.

6. Conclusion

We propose a fully distributed, auctioneer-free, hierarchical auction method for wireless resource allocation in local Power AIoT. In the upper tier, we employ a multi-hop progressive auction to address slicing resource allocation between MNOs and MVNOs. In the lower tier, a benefit optimization-based strategy allocates time–frequency resource blocks between MVNOs and power terminals. Simulation results show that the social welfare of MPAA decreases with incremental bid evaluation, with shorter convergence. MPAA achieves the highest social welfare and reduces the bidding overhead of MVNOs by 6.12%. TRAS exhibits faster convergence, increasing terminal satisfaction in private edge cloud systems.

CRediT authorship contribution statement

Yuhuai Peng: Funding acquisition. **Jing Wang:** Writing – original draft. **Xiongang Ye:** Writing – original draft, Conceptualization. **Fazlullah Khan:** Writing – review & editing, Validation, Formal analysis. **Ali Kashif Bashir:** Software, Investigation. **Bandar Alshawi:** Data curation. **Lei Liu:** Supervision. **Marwan Omar:** Visualization, Software.

Declaration of competing interest

The authors declared that they have no conflicts of interest to this work.

Data availability

No data was used for the research described in the article.

References

[1] N. Khan, S.U. Khan, F.U.M. Ullah, M.Y. Lee, S.W. Baik, AI-assisted hybrid approach for energy management in IoT-based smart microgrid, IEEE Internet Things J. 10 (21) (2023) 18861–18875.

[2] Y. Ye, L. Shi, X. Chu, R.Q. Hu, G. Lu, Resource allocation in backscatter-assisted wireless powered MEC networks with limited MEC computation capacity, IEEE Trans. Wireless Commun. 21 (12) (2022) 10678–10694.

[3] J.J. Park, J.H. Moon, H.H. Jang, D.I. Kim, Unified simultaneous wireless information and power transfer for IoT: Signaling and architecture with deep learning adaptive control, IEEE Internet Things J. 9 (18) (2022) 17551–17567.

[4] S. D'Oro, F. Restuccia, A. Talamonti, T. Melodia, The slice is served: Enforcing radio access network slicing in virtualized 5G systems, in: IEEE INFOCOM 2019-IEEE Conference on Computer Communications, IEEE, 2019, pp. 442–450.

[5] X. Zhang, Q. Zhu, Game-theory based power and spectrum virtualization for optimizing spectrum efficiency in mobile cloud-computing wireless networks, IEEE Trans. Cloud Comput. 7 (4) (2017) 1025–1038.

[6] X. Chen, Z. Han, H. Zhang, G. Xue, Y. Xiao, M. Bennis, Wireless resource scheduling in virtualized radio access networks using stochastic learning, IEEE Trans. Mob. Comput. 17 (4) (2017) 961–974.

[7] H. Li, H. Li, X. Wen, L. Wang, Z. Lu, W. Jing, Y. Chen, An interference minimization-based RAN slicing strategy in 5G systems, in: 2021 17th International Symposium on Wireless Communication Systems, ISWCS, IEEE, 2021, pp. 1–6.

[8] Q. Kuang, W. Utschick, A. Dotzler, Optimal joint user association and multi-pattern resource allocation in heterogeneous networks, IEEE Trans. Signal Process. 64 (13) (2016) 3388–3401.

[9] M. Jiang, M. Condoluci, T. Mahmoodi, Network slicing in 5G: An auction-based model, in: 2017 IEEE International Conference on Communications, ICC, IEEE, 2017, pp. 1–6.

[10] L. Liu, J. Feng, X. Mu, Q. Pei, D. Lan, M. Xiao, Asynchronous deep reinforcement learning for collaborative task computing and on-demand resource allocation in vehicular edge computing, IEEE Trans. Intell. Transp. Syst. 24 (12) (2023) 15513–15526.

[11] A. Alsharoa, M.-S. Alouini, Improvement of the global connectivity using integrated satellite-airborne-terrestrial networks with resource optimization, IEEE Trans. Wireless Commun. 19 (8) (2020) 5088–5100.

[12] P. Qin, Y. Fu, X. Zhao, K. Wu, J. Liu, M. Wang, Optimal task offloading and resource allocation for C-NOMA heterogeneous air-ground integrated power internet of things networks, IEEE Trans. Wireless Commun. 21 (11) (2022) 9276–9292.

[13] N. Raveendran, Y. Gu, C. Jiang, N.H. Tran, M. Pan, L. Song, Z. Han, Cyclic three-sided matching game inspired wireless network virtualization, IEEE Trans. Mob. Comput. 20 (2) (2019) 416–428.

[14] P. Qin, M. Wang, X. Zhao, S. Geng, Content service oriented resource allocation for space–air–ground integrated 6G networks: A three-sided cyclic matching approach, IEEE Internet Things J. 10 (1) (2022) 828–839.

[15] C.V. Nahum, V.H. Lopes, R.M. Dreifuerst, P. Batista, I. Correa, K.V. Cardoso, A. Klautau, R.W. Heath, Intent-aware radio resource scheduling in a ran slicing scenario using reinforcement learning, IEEE Trans. Wireless Commun. (2023).

[16] M. Zhang, Y. Dou, V. Marojevic, P.H.J. Chong, H.C. Chan, FAQ: A fuzzy-logic-assisted Q learning model for resource allocation in 6G V2X, IEEE Internet Things J. (2023).

[17] J. Tian, Q. Liu, H. Zhang, D. Wu, Multiagent deep-reinforcement-learning-based resource allocation for heterogeneous QoS guarantees for vehicular networks, IEEE Internet Things J. 9 (3) (2021) 1683–1695.

[18] W. Lei, Y. Ye, M. Xiao, Deep reinforcement learning-based spectrum allocation in integrated access and backhaul networks, IEEE Trans. Cogn. Commun. Netw. 6 (3) (2020) 970–979.

[19] S. Wang, M. Chen, X. Liu, C. Yin, S. Cui, H.V. Poor, A machine learning approach for task and resource allocation in mobile-edge computing-based networks, IEEE Internet Things J. 8 (3) (2020) 1358–1372.

[20] F. Li, Z. Xu, H. Li, A multi-agent based cooperative approach to decentralized multi-project scheduling and resource allocation, Comput. Ind. Eng. 151 (2021) 106961.

[21] X. Hu, Y. Wang, Z. Liu, X. Du, W. Wang, F.M. Ghannouchi, Dynamic power allocation in high throughput satellite communications: A two-stage advanced heuristic learning approach, IEEE Trans. Veh. Technol. 72 (3) (2022) 3502–3516.

[22] F.d.O. Torres, V.A.S. Júnior, D. da Costa, D.L. Cardoso, R.C. Oliveira, Radio resource allocation in a 6G D-OMA network with imperfect SIC: A framework aided by a bi-objective hyper-heuristic, Eng. Appl. Artif. Intell. 119 (2023) 105830.

[23] L.X. Nguyen, Y.K. Tun, T.N. Dang, Y.M. Park, Z. Han, C.S. Hong, Dependency tasks offloading and communication resource allocation in collaborative UAVs networks: A meta-heuristic approach, IEEE Internet Things J. (2023).

[24] M. Katwe, K. Singh, C.-P. Li, Z. Ding, Ultra-high rate-reliability fairness in grant-free massive URLLC NOMA system: Joint power and channel allocation using meta-heuristic search, IEEE Trans. Veh. Technol. (2023).

[25] X. Zhang, K. An, B. Zhang, Z. Chen, Y. Yan, D. Guo, Vickrey auction-based secondary relay selection in cognitive hybrid satellite-terrestrial overlay networks with non-orthogonal multiple access, IEEE Wirel. Commun. Lett. 9 (5) (2020) 628–632.

[26] P.-Y. Su, K.-H. Lin, Y.-Y. Li, H.-Y. Wei, Priority-aware resource allocation for 5G mmWave multicast broadcast services, IEEE Trans. Broadcast. 69 (1) (2022) 246–263.

[27] I. Yadav, A.A. Kulkarni, A. Karandikar, Strategy-proof spectrum allocation among multiple operators in wireless networks, IEEE Trans. Veh. Technol. 69 (12) (2020) 15964–15977.

[28] R. Zhu, H. Liu, L. Liu, X. Liu, W. Hu, B. Yuan, A blockchain-based two-stage secure spectrum intelligent sensing and sharing auction mechanism, IEEE Trans. Ind. Inform. 18 (4) (2021) 2773–2783.

[29] S. Hosseinalipour, H. Dai, A two-stage auction mechanism for cloud resource allocation, IEEE Trans. Cloud Comput. 9 (3) (2019) 881–895.

[30] X. Zhang, D. Guo, K. An, G. Zheng, S. Chatzinotas, B. Zhang, Auction-based multichannel cooperative spectrum sharing in hybrid satellite-terrestrial IoT networks, IEEE Internet Things J. 8 (8) (2020) 7009–7023.

[31] V. Jumba, S. Parsaeefard, M. Derakhshani, T. Le-Ngoc, Dynamic resource provisioning with stable queue control for wireless virtualized networks, in: 2015 IEEE 26th Annual International Symposium on Personal, Indoor, and Mobile Radio Communications, PIMRC, 2015, pp. 1856–1860.

[32] S. D'Oro, F. Restuccia, A. Talamonti, T. Melodia, The slice is served: Enforcing radio access network slicing in virtualized 5G systems, in: IEEE INFOCOM 2019 - IEEE Conference on Computer Communications, 2019, pp. 442–450.

[33] W. Zhong, K. Xie, Y. Liu, C. Yang, S. Xie, Multi-resource allocation of shared energy storage: A distributed combinatorial auction approach, IEEE Trans. Smart Grid 11 (5) (2020) 4105–4115.

[34] S. Mirjalili, S.M. Mirjalili, A. Lewis, Grey wolf optimizer, Adv. Eng. Softw. 69 (2014) 46–61.

[35] R. Zheng, An improved discrete particle swarm optimization for airline crew rostering problem, in: 2020 IEEE Congress on Evolutionary Computation, CEC, 2020, pp. 1–7.
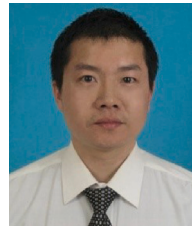
Yuhuai Peng received the Ph.D. degree in communication and information systems from Northeastern University in 2013. He is now a professor in the same university. His research interests include Internet of Things (IoT), Communication Physical Systems (CPS), Digital Twins, Metaverse, etc. (email: pengyuhuai@mail.neu.edu.cn).

Jing Wang received the M.E. degree in Electronic Science and Technology from Yanshan University, Qinhuangdao, China, in 2020. She is currently working toward the Ph.D. degree in the School of Computer Science and Engineering at Northeastern University, Shenyang, China. Her research interests edge computing, Digital Twins and Metaverse. (email: 2110651@stu.neu.edu.com).
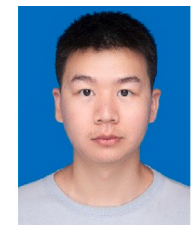
Xiong'ang Ye received the B.S degree from Hebei University of Engineering in 2020, majoring in communication engineering. He received the master's degree in the School of Computer Science and Engineering at Northeastern University, Shenyang, China, in 2023. His research interests are power wireless communication, 5G network slicing. (email: yxa337115654@163.com).

Fazlullah Khan Fazlullah Khan (SMIEEE) got Ph.D. in Computer Science from AWKUM in 2020. He is working in the School of Computer Science, Faculty of Science and Engineering, University of Nottingham Ningbo China, Zhejiang, China. He is listed in the top 2% scientists of in the World. His research interest is AI, security, intelligent systems, IoT, and health informatics (email: fazl.ullah@nottingham.edu.cn).

Ali Kashi Bashir is a Professor at the Department of Computing and Mathematics, Manchester Metropolitan University, UK. He is the leader of Secure and Intelligent Systems Research Group; Future Networks Lab and IoT/Cybersecurity Testbed. Throughout his career, Ali has presented more than 50 keynote speeches on an international scale and produced over 300 research articles. He has obtained over £4 million in external funding from UK, South Korean, Japanese, European, Asian, and Middle Eastern agencies. His students have won best paper awards, best Ph.D. thesis awards, and several other recognitions. He is a senior member of IEEE, a member of several technical societies, and a Distinguished Speaker of ACM. He received the Clarivate Highly Cited Researcher Award in 2023. He was listed as an IEEE Featured Author in 2021, and highly cited 2% of researchers by Stanford University in 2021 and 2022. He is EIC of IEEE Technology, Policy and Ethics, and Journal of Autonomous Intelligence, Vetting Advisory Committee Member of IEEE Transactions on Consumer Electronics, and AE of IEEE Transactions on Network Science and Engineering. (email: dr.alikashif.b@ieee.org).

Bandar Alshawi received the Ph.D. in computer engineering from Florida institute of Technology Melbourne, FL, USA. He is currently an assistant professor in the department of computer and network engineering, college of computing, Umm Al-Qura University, Makkah, Saudi Arabia. His research interests includes: artificial intelligence, internet of things, cybersecurity. (email: bmhshawi@uqu.edu.sa).

Lei Liu received the B.Eng. degree in communication engineering from Zhengzhou University, Zhengzhou, China, in 2010, and the M.Sc. and Ph.D degrees in communication engineering from Xidian University, Xian, China, in 2013 and 2019, respectively. From 2013 to 2015, he was employed a subsidiary of China Electronics Corporation. From 2018 to 2019, he was supported by China Scholarship Council to be a visiting Ph.D. student with the University of Oslo, Oslo, Norway. He is currently an Associate Professor with the Guangzhou Institute of Technology, Xidian University. His research interests include vehicular ad hoc networks, intelligent transportation, mobile-edge computing, and Internet of Things (email: leiliu@xidian.edu.cn).

Marwan Omar received a Master's degree in Information Systems and Technology from the University of Phoenix, 2009 and a Doctorate Degree in Digital Systems Security from Colorado Technical University, 2012. He is currently an associate professor at Illinois Institute of Technology where he teaches cyber security and digital forensics courses. His research interests fall in the broad area of cyber security with a recent focus on machine learning robustness. Among other services, he is currently an active reviewer for IEEE Access, IEEE Transactions on Parallel and Distributed Systems and a member of IEEE since 2021. (email: momar3@iit.edu).